NASA PRE-EVENT DEBRIS FOOTPRINT ESTIMATES FOR THE DEORBIT OF SPACE STATION MIR

Richard B. Mrozinski

NASA Johnson Space Center
Flight Design and Dynamics Division, Mail Code: DM4
2101 NASA Road 1, Houston, Texas, 77058, USA
richard.b.mrozinski1@jsc.nasa.gov

ABSTRACT

This paper details a method used by the National Aeronautics and Space Administration (NASA) Johnson Space Center to estimate the size and location of the debris footprint expected from the entry and breakup of the Mir Space Station, and results of this method obtained prior to the event. The method estimates the length (range), width (crossrange), and location of debris splashdown and breakup footprints. The method utilizes a three degree-of-freedom Monte Carlo simulation incorporating uncertainties in all aspects of the problem, including vehicle and environment uncertainties. The method incorporates a range of debris characteristics based on historical data in addition to any vehicle-specific debris catalog information.

1. OVERVIEW

Although the Russian government maintained sole responsibility for the deorbit planning and operations, Russia requested international assistance in obtaining orbital tracking data. The U.S., while maintaining its position as an observer of this event, agreed to provide tracking data where possible through the National Aeronautics and Space Administration (NASA) Mission Control Center in Houston. In addition to tracking support, NASA performed two independent assessments: orbital decay predictions and footprint analyses. This paper presents methods and results of the debris footprint analyses completed prior to the deorbit of Space Station Mir on March 23, 2001.

2. UNITS, CONVENTIONS, AND SYMBOLS

Values in this paper are presented in standard SI units. All calculations were done in English Engineering System units. All longitudes are provided as positive Eastward from Greenwich. All latitudes are geodetic and are provided as positive northward from the equator. Symbols used are as follows:

C_d Effective average drag coefficient (Eq. 1)
L/D Effective average lift-to-drag ratio
m Effective average mass (Eq. 1)
S Effective average, or reference, aerodynamic surface area (Eq. 1)
β Effective average ballistic coefficient (Eq. 1)
σ One standard deviation of sample output data

3. METHOD OVERVIEW

A three degree-of-freedom simulation was built using version 8.05 of the Simulation and Optimization of Rocket Trajectories [1] program at JSC. The simulation was built assuming an instantaneous breakup of the Mir vehicle at a given altitude, not a multiple-stage breakup over an altitude region. The intact Mir vehicle was modelled as a point mass (constant orientation), with constant aerodynamic and mass properties. The assumption of constant mass was acceptable as there are no significant mass or shape changes prior to breakup. The assumption of constant aerodynamics was also valid, as the aerodynamic coefficients used here were intended to represent equivalent average values. Additionally, it has been shown that the regime in which drag coefficient changes significantly occurs after the debris achieves vertical flight, and therefore has no impact on footprint size [2]. The constant orientation assumption had no impact since no lift was modelled prior to breakup.

Beginning at the breakup altitude, the simulation then modelled a single debris piece down to an altitude of 15.24 km, which was considered as ground impact. At the breakup altitude, an instantaneous change in mass, aerodynamics, and bank angle were modelled, all of which were then held constant to ground impact. Holding the bank angle constant was not overly conservative because a reduced lift-to-drag ratio was used which assumed a constant bank orientation [3]. The assumption of constant mass and aerodynamics was erroneous in reality due to the ablation of debris pieces through their entry. However, in modelling the debris here, the ballistic coefficients used were intended to represent equivalent average values, rather than the actual indeterminable values.

Although a hydrazine explosion was a possible breakup scenario, it was ignored here for two reasons. First, any explosion would have been nearly impossible to model with any certainty without performing a detailed blast analysis. Second, regardless of any answers that such an analysis would have produced, the most that could be done to protect for public safety was done by Russia by targeting the footprint in the middle of the available ocean area as much as possible.

Using nominal vehicle properties and assuming no breakup, an intact reference trajectory and corresponding impact point for the intact vehicle were determined. This point was not very realistic, as a breakup was guaranteed, but provided a good reference point. Monte Carlo (MC) methods were also needed to account for all non-linearities and the large number of variables involved. This method used the 1999 Global Reference Atmosphere Model (GRAM-99) and localized winds. The Monte Carlo runs included variations in: drag coefficient, lift coefficient, reference aerodynamic surface area, and mass for both the intact vehicle before breakup and the debris pieces after vehicle breakup. All variations were distributed in a uniform distribution, to be most conservative. Five hundred cases were run, producing five hundred impact points. Initial condition uncertainties were not used at all in the Monte Carlo study. Rather, various overburn and underburn initial condition vectors were generated, then each studied individually. This variety of initial conditions was assumed to provide enough information to cover all uncertainties in the initial conditions.

4. MODELS AND ASSUMPTIONS

Here, various models are described as well as the assumptions involved. Since the footprint was planned for an open ocean area, we were conservative in this analysis wherever possible and reasonable.

4.1 Integration Method

A fourth-order Runge-Kutta method was used to integrate the equations of motion. An integration step size of one second was used throughout the trajectory, except for five seconds beginning at breakup where the step size was reduced to 0.01 second. This reduction was used to allow the dynamics to adjust to instantaneous changes in mass and aerodynamics. Integration method effects on the footprint were assumed minimal, and were not investigated further.

4.2 Planet and Gravity Models

The planet model used in this study was an oblate spheroid Earth, set by the equatorial and polar radii [1]. The polar axis was considered an axial axis of symmetry, and was assumed to be the planet's rotational axis. The gravitational model consisted of the central gravitational force adjusted via the first three oblate zonal harmonic coefficients (J2, J3, and J4) [1]. Planet and gravity model variations were assumed to have minimal effect on the resulting footprint, and were not investigated further.

4.3 Atmosphere Model

Experience with the methods used here has shown that winds have significant impact on the width of the footprint (more pronounced near the heel, or least-range-flown part of the footprint), but negligible impact on the footprint's length characteristics cases [4]. Thus, our Monte Carlo method used the GRAM-99 atmosphere model and wind database, which models localized winds, density, density variations and shears, and solar activity effects. (GRAM localizes density perturbations and winds, such that they are specific to the latitudinal and longitudinal position, as well as altitude, month, etc.) Here, GRAM was used with an entry date of March 23, 2001, and the actual solar activity values for mean solar 10.7 cm radio noise flux and geomagnetic index on March 23 [5,6].

4.4 Guidance, Navigation, and Control

The guidance, navigation, and control (GN&C) system was disabled, as the vehicle would be in a completely uncontrolled trajectory during entry.

4.5 Aerodynamics and Mass Properties

Ideally, we would input into the simulation only the ballistic coefficient (β) and lift-to-drag ratio (L/D). However, SORT requires mass properties for simulation, therefore we had to provide each component of the ballistic coefficient: drag coefficient (C_d), reference aerodynamic surface area (S), and mass (m). Note that designating values of these latter three variables was arbitrary, since when the lift is zero it is only the ballistic coefficient that dictates the trajectory of the vehicle or debris. Here, ballistic coefficient is defined as in Eq. 1.

$$\beta = m/(SC_d) \qquad (1)$$

We now discuss the aerodynamic and mass properties used in this study beginning with the properties of the intact (pre-breakup) Mir. We will then move to the post-breakup debris properties.

4.5.1 Intact Mir Characteristics

We first selected a range of ballistic coefficients for the intact Mir vehicle, then selected appropriate values of mass, drag coefficient, and aerodynamic surface area

that produced the limits of that range. The values that were selected were arbitrary, as long as the resulting ballistic coefficients were correct. We could do this because although the author was not aware of any plans to intentionally induce tumbling of Mir after its final deorbit burn, we were virtually guaranteed tumbling of Mir as it entered the upper atmosphere. Thus *L/D* was going to be effectively zero, and the ballistic coefficient therefore would entirely determine the trajectory prior to breakup.

For intact ballistics, we began with a drag coefficient (C_d) of 2.0, an aerodynamic cross-sectional surface area of 392.5 m^2, and a total wet mass of 135256.8 kg according to trajectory curve-fits by the International Space Station Trajectory Officers at NASA JSC on March 21, 2001 [5]. These values led to a ballistic coefficient of 172.3 kg/m^2. For orbital decay predictions, Russia supplied a ballistic coefficient range of 188.6 – 350.2 kg/m^2 [7]. To bound these values and to be conservative, we selected a ballistic coefficient range of 146.5 - 366.2 kg/m^2.

The actual reentry mass of Mir was extremely difficult to predict due to uncertainties in the burn plan. Luckily, only the ballistic coefficient was important, and as such we were able to arbitrarily select an entry mass. Another mass value seen was 122470.0 kg [8], which the author believed was only a rough estimate. To be in the overall ballpark, here the mass was set to 127006.0 kg. Similarly, we were able to arbitrarily set the drag coefficient. The only value available, which is what we used, was the value provided by the ISS Trajectory Officers (as above) of 2.0.

Finally, after "arbitrarily" setting mass and drag, we had to set the aerodynamic cross-sectional surface area to achieve the desired ballistic coefficient range. Using the above values, this resulted in an area of 173.4 - 433.6 m^2. For comparison, the Russians provided an overall range of on-orbit cross-sectional areas of 50.0 – 455.0 m^2 [8]. We were comfortable with a tighter range for this study, because this reduced range was appropriate for a tumbling vehicle.

To reiterate, we assumed the vehicle would tumble as it entered the upper atmosphere, down through to breakup, so pre-breakup *L/D* was zero. (Previous experience indicates that *L/D* prior to breakup has negligible impact on debris footprints for objects that break up above 74 km [4]).

The intact (reference) mass and aerodynamic properties are summarized in Table 1. Note that in determining this reference impact point, it was assumed that no vehicle breakup would occur. Note that the aerodynamic reference area was set to the mid-point of the range above. The resulting Monte Carlo data from the above assumptions is given in Table 2.

Table 1. Intact (Reference) Mass and Aerodynamic Data, Intact Mir Vehicle

Variable	Intact (Reference) Value
Mass	127006.0 kg
Drag Coefficient	2.0
Aerodynamic Surface Area	303.5 m^2
Ballistic Coefficient	209.3 kg/m^2
L/D Ratio	0.0
Lift Coefficient	0.0

Table 2. Monte Carlo Mass and Aerodynamic Data, Intact Mir Vehicle

Variable	Mean Value	Dispersion Limit (Uniform Distribution)
Mass	127006.0 kg	± 0.0 kg
Drag Coefficient	2.0	± 0.0
Aerodynamic Surface Area	303.5 m^2	± 130.1 m^2
L/D Ratio	0.0	± 0.0

4.5.2 Post-Breakup Debris Characteristics

It is always impossible to say with any certainty exactly what any of debris pieces will look like and what characteristics they will have for any entry event. Therefore, our approach involved arriving at assumptions for a "generic" (or "general") debris field's ballistic and lift coefficients, by surveying previous disposal analyses for historical data. Once settled on a range of general debris characteristics, we examined the vehicle for any particular debris pieces that actually might be identifiable to some extent, that could exist after breakup and survive entry. If any of these pieces existed outside the historical range we selected for "general" or "generic" debris, then separate studies would be done focusing on just those unique pieces. Next, we examined the vehicle for any particular debris pieces that might separate from the main vehicle at an altitude significantly higher than the estimated breakup altitude. If any of these could be identified, then separate studies would be done focusing just on those items. Here, it turned out that we ended up modelling three distinct debris fields: general debris, film safe debris (single piece), and solar array (and other appendages) debris.

We begin with determining a range of ballistic coefficients for the general debris field. Before proceeding, note that Russian ballistics experts stated that the range they were using for footprint analyses was 16.4 – 1635.7 kg/m^2 [9].

For the general debris field, we rely on historical data from previous analyses. Some ballistic coefficient

ranges used in previous studies for various vehicles are shown in Table 3. After checking with one of the original authors (McCormick) of the source of the Skylab data, it was concluded that the maximum ballistic coefficient of 1562.4 kg/m^2 used in Skylab analyses is much too high for typical vehicles, as this value corresponded to an aluminum film safe onboard Skylab, and values of no greater than 684 kg/m^2 should be used for typical debris items. Mr. McCormick continued to say that this would provide about the right amount of conservatism if a purely ballistic trajectory is modelled after breakup; if *L/D* is modelled, he suggested that 684 kg/m^2 would be excessively conservative as it is very unusual to get a debris pieces above 490 kg/m^2 [10].

Table 3. Debris Ballistic Coefficient Ranges for Previous Disposal Analyses [11]

Reentry Vehicle	Ballistic Coefficient Range
Space Shuttle External Tank	13.7 – 283.2 kg/m^2
Apollo Service Module	2.4 - 463.8 kg/m^2
Soyuz Service Module	6.8 – 566.4 kg/m^2
Skylab	4.9 - 1562.4 kg/m^2

Based on this, and since this study did model post-breakup *L/D*, we determined that a high-end ballistic coefficient for the general debris field should be around 490 kg/m^2. We used 566.4 kg/m^2 as this was the highest number seen in previous analyses (excluding the Skylab film safe), and added some conservatism. Why then did the Russians quote such a high ballistic coefficient for their maximum? Like Skylab, the Mir Kvant module also had an aluminum film safe that was very likely to survive entry [12]. It was then assumed that this piece defined the Russian upper limit of 1635.7 kg/m^2 (which is about the same as for the film safe on Skylab), and further assumed that there was very little likelihood of any debris items existing between 566.4 kg/m^2 and 1635.7 kg/m^2. Therefore, we now were examining two debris groups: general debris and film safe debris. Our upper limit of ballistic coefficients was therefore 566.4 kg/m^2 for general debris, and the film safe debris was modelled at a constant 1635.7 kg/m^2.

In selecting the low end for the general debris, we felt the lowest value in Table 3 to be adequately conservative since any identifiable pieces of less than this value would have the lowest capability of all the pieces to cause damage. Thus, we adopted the range of 2.4 – 463.8 kg/m^2 for general debris.

At this point, we had a ballistic coefficient range based on historical data, and examined the debris catalogue for pieces which may be beyond this range, leaving us with two debris fields: general (2.4 – 463.8 kg/m^2) and film safe (constant 1635.7 kg/m^2) debris fields. We now turn to items that may separate, or break off of the main body prior to breakup. Generally this is expected to occur for solar arrays and other appendages. Mir did have many solar arrays and appendages; therefore we needed a third debris field to study. For the solar array debris field, we assumed a ballistic coefficient range of 9.8 – 19.5 kg/m^2.

Given these ranges of ballistic coefficients, we then had to select appropriate values of mass, drag coefficient, and aerodynamic surface area which produced the limits of this ranges. The values that were selected were arbitrary, as long as the resulting ballistic coefficients were correct. For all debris, we arbitrarily selected a drag coefficient of 1.0. We then selected constant mass values of 22.7 kg, 90.7 kg, and 226.8 kg for the general, solar array, and film safe debris fields, respectively. Then, by selecting an aerodynamic reference area range of 0.04 - 9.29 m^2 for the general debris arrived at the desired ballistic coefficient range of 2.4 – 566.4 kg/m^2. By selecting an aerodynamic reference area range of 4.65 – 9.29 m^2 for the solar array debris arrived at the desired ballistic coefficient range of 9.8 – 19.5 kg/m^2. Finally, by selecting a constant aerodynamic reference area of 0.14 m^2 for the film safe debris arrived at the desired constant ballistic coefficient of 1635.7 kg/m^2.

Next, we had to select ranges of lift-to-drag ratios for the three debris fields. A maximum ratio of 0.15 was found in studies done for the Soyuz launch vehicle [11]. Although debris pieces generally can exhibit higher *L/D* values, they were unlikely to hold the lift vector in a constant orientation as we modelled here. The 0.15 value used is a reduced *L/D* that applies when constant bank angles are used [3]. Since we assumed that the pieces of debris will neither trim at a stable orientation, nor tumble at a high enough rate to generate substantial lift, then were then able to assume a lift-to-drag ratio in the range of 0.0 - 0.15, for all debris. (If this study were repeated, the author would use a constant *L/D* of zero for the film safe, as objects of that general shape would not lead to significant lift.)

For the three debris field Monte Carlo sets, the means of the data presented above were used, and the dispersions were set to the difference between the means and the extremes. The resulting Monte Carlo data is given in Tables 4, 5, and 6, for the general, film safe, and solar array debris fields, respectively.

4.6 Initial State

The nominal (23.5 m/sec) post-final-burn state vector used in this study was received from the Russian Ballistics group by the JSC Trajectory Operations Officer (TOPO), who converted it to the parameters

and values shown in Table 7 before forwarding to the author [6]. The TOPO also modelled the final burn to produce overburn and underburn vectors, at 1 m/sec intervals, from a 4 m/sec overburn down to a 7 m/sec underburn [6]. This wide variation in burn dispersions was assumed to be of much larger magnitude than all other possible uncertainties in the initial state, so the twelve burn 3 cutoff vectors were used with no uncertainties added.

Table 4. Monte Carlo Mass and Aerodynamic Data, General Debris

Variable	Mean Value	Dispersion Limit (Uniform Distribution)
Mass	22.7 kg	± 0.0 kg
Drag Coefficient	1.0	± 0.0
Aerodynamic Surface Area	4.67 m^2	± 4.63 m^2
L/D Ratio	0.075	± 0.075
Bank Angle	0.0 deg	± 180.0 deg

Table 5. Monte Carlo Mass and Aerodynamic Data, Film Safe Debris Only

Variable	Mean Value	Dispersion Limit (Uniform Distribution)
Mass	226.8 kg	± 0.0 kg
Drag Coefficient	1.0	± 0.0
Aerodynamic Surface Area	0.14 m^2	± 0.0 m^2
L/D Ratio	0.075	± 0.075
Bank Angle	0.0 deg	± 180.0 deg

Table 6. Monte Carlo Mass and Aerodynamic Data, Solar Array Debris Only

Variable	Mean Value	Dispersion Limit (Uniform Distribution)
Mass	90.7 kg	± 0.0 kg
Drag Coefficient	1.0	± 0.0
Aerodynamic Surface Area	6.97 m^2	± 2.32 m^2
L/D Ratio	0.075	± 0.075
Bank Angle	0.0 deg	± 180.0 deg

Table 7. Nominal Burn 4 Cutoff Vector as of 0247 CST March 22, 2001 (Last pre-burn update) [6]

Variable	Value
Longitude	121.858548 deg
Geodetic Latitude	41.983217 deg
Geodetic Altitude	177.3381675 km
Inertial Speed	7788.691347 m/sec
Inertial Flight Path Angle	-0.491694 deg
Inertial Azimuth Angle	123.6158 deg

Here, "nominal" refers to a 23.5 m/sec final burn. However, note that Russia was planning to burn the engines in this last maneuver to depletion, and therefore an overburn in this case is also "nominal", in other words an overburn is not a failure scenario as might be normally thought. Here, we refer to the 23.5 m/sec burn as nominal, and anything more as an overburn, and anything less as an underburn. Only underburns are failure scenarios.

4.7 Termination Conditions

All simulations (reference intact and Monte Carlo) were terminated at an altitude of 15.24 km. This has been done for other programs and was done here. As an example, a TRW analysis of the debris footprint resulting from the reentry of the Compton Gamma Ray Observatory (CGRO) showed that errors on the order of 0.1 degree in latitude and longitude resulted by stopping at 50 km rather than 1 km [13]. Regardless, we terminated at 15.24 km, which we determined to be approximately the lowest the simulation can go on heel debris pieces without encountering chaotic wind impacts on heel pieces in near vertical flight. Additionally, the termination altitude of 15.24 km has been used in other footprint studies, such as for the Space Shuttle Super Lightweight External Tank [11].

4.8 Breakup Model

Breakup was assumed to occur at a single discrete altitude for modelling purposes. In reality breakup always occurs in multiple stages over an altitude range. Additionally, ablation can create a near-constant stream of new debris over a very large altitude range. It was impossible to predict or model the actual stages of breakup or when they will occur. Therefore, we modelled the entire breakup at an altitude high enough to be conservative (higher breakup altitudes generally lead to larger debris footprints). Entry tests show that typical satellites of aluminum or magnesium structure will breakup up around 77.8 km [14]. Results of breakup analyses' predictions and/or observations for various vehicles are shown in Table 8 [11]. Preflight footprint analyses for the deorbit of the CGRO assumed a breakup at 83.8 km [13,15], where actual breakup occurred at 72.2 km [16].

The Russians predicted the primary breakup to occur from 80 – 90 km, and the solar arrays to break off of the primary structure from 100 – 110 km [7,8,17].

Having looked at Table 8 and considered the typical value of 77.8 km, we see the Russian estimates for the primary breakup of 90.0 km (max, to be conservative) to be higher than the 77.8 km typical value, and higher than all table values, except for the assumed values for

the Super Lightweight tank and the 94.5 km value for Skylab, which is very high. Therefore, we used the same breakup altitude as proposed by Russia, 90.0 km, as this high value was conservative.

Table 8. Breakup Altitudes Found in Previous Disposal Analyses and Observations [11]

Reentry Vehicle	Breakup Altitude
Space Shuttle External Tank (Actual Results)	61.1 - 83.3 km
Space Shuttle Super Lightweight Tank (Assumed)	61.1 - 88.9 km
Soyuz Service Module	64.8 - 83.3 km
VAST/VASP	77.8 km
Apollo Service Module	83.3 km
Skylab	77.8 - 94.5 km
Compton Gamma Ray Observatory	72.2 km

5. MIR DEBRIS FOOTPRINT ESTIMATES

Here we present the results of the Monte Carlo study. All times are calculated relative to the reference cutoff of the nominal 23.5 m/sec final burn, of 05:27:02.883 GMT on March 23, 2001 [6]. All range values are calculated with respect to one of two arbitrary reference points: the crossing of the orbit groundtrack (as determined by the initial conditions) with either the east coast of Asia (Japan) or the west coast of South America (Chili). These two reference points are shown in Table 9. Thus, a range value of 2000 km indicates either a location 2000 km east of Japan or west of Chili along the orbit groundtrack. A negative value would indicate that the footprint has crossed the coastline and debris may fall on land. The crossrange was calculated with respect to the initial orbital plane frozen at the vector time. A positive value indicates the debris landed to the right of the orbital plane (in this case south of the entry groundtrack).

Table 9. Reference Points for Range Values

Case	Asia Eastern Coast Crossing (Japan)	South America Western Coastal Crossing (Chili)
Geodetic Latitude	33.6°	-43.8°
Longitude	134.6°	-73.0°

5.1 Nominal Burn Results

Monte Carlo simulations were run first for the nominal burn scenario. For the nominal burn, separate results were obtained for the general, film safe, and solar array debris fields.

First, we present results in Table 10 for Entry Interface (EI), defined at 121.9 km, the falloff of the solar arrays and other appendages at 110.0 km as per the Russian maximum solar array breakoff altitude estimate, the beginning of breakup at 90.0 km as per the Russian maximum breakup altitude estimate, and the "end" of breakup at 77.8 km which is the author's best educated guess at the primary breakup altitude.

Table 10. Various Event Predictions During Entry, Nominal Final Burn

Event	Geodetic Latitude (deg)	Longitude (deg)	Time wrt Burn Cutoff (min)
EI	10.14 N	156.06 E	11.0
Solar Array Breakoff	0.64 ± 0.04 N	162.91 ± 0.05 E	13.9
Main Body Breakup, Start	23.16 ± 2.6 S	178.78 ± 0.80 W	21.3
Main Body Breakup, "End"	34.06 ± 6.4 S	167.24 ± 8.1 W	25.0

Results of the Monte Carlo study for the nominal final deorbit burn are shown in Table 11 for the three debris footprints. Note that of the 500 Monte Carlo cases ran, zero percent skipped out.

The impact distribution along the width of the footprint was computed assuming a nominal, or Gaussian, distribution centered about the groundtrack. 3σ values are presented in the results. The distribution along the length of the footprint is not Gaussian in nature. Therefore, length was computed using statistics theory for general distributions, whereby taking the maximum and minimum range values for the sample size of 500 leads to bounding points which theory states provide enough protection to bound 98% of impact points with 95% confidence [18].

For the nominal burn scenario, we see a footprint whose geometric center is 10540 km downrange of the east coast of Japan, and whose closest approach to Japan's east coast is 7050 km. Also, the closest approach to Chili's west coast is 3360 km. The footprint is 6980 km long, 390 km wide. The Monte Carlo impact points accounting for all three debris fields are coplotted in Fig. 1.

Table 11. Nominal Final Burn Monte Carlo Results

Statistic	General Debris	All Debris
Length	3300 km	6980 km
Width	390 km	390 km
Center w.r.t. Japan	9930 km	10540 km
Heel w.r.t. Japan	8270 km	7050 km
Toe w.r.t. Chili	5820 km	3360 km
Min Time to 15.24 km	27.2 min	24.8 min
Max Time to 15.24 km	38.8 min	38.8 min

Also of interest as part of the nominal burn predictions was where, in terms of latitude and longitude, would the fall-off or break-off of the solar arrays occur, and

where would general (main vehicle) breakup occur. For these estimates lying in the Eastern and Western Hemispheres, see Figs. 2 and 3, respectively. Fig. 2 shows solar array and other appendages fall-off as depicted by Item A, based on the maximum break-off estimates by the Russians for the solar arrays (break-off at 110 km). Item B in Figs 2 and 3 shows where breakup was expected based on the maximum general breakup estimate by the Russians (breakup at 90 km). Item C in Fig. 3 shows where breakup was expected based on the author's best educated guess at the primary breakup altitude (breakup at 77.8 km).

5.2 Off-Nominal Burn Results

Monte Carlo simulations were run for a range of overburn and underburns, in 1 m/sec increments, from a 4 m/sec overburn to a 7 m/sec underburn. For all burns, separate results were obtained for the general, film safe, and solar array debris fields.

Results of the Monte Carlo study for an off-nominal, 4 m/sec overburn on the final deorbit burn are shown in Table 12 for the three debris footprints. The Monte Carlo impact points accounting for all three debris fields are coplotted in Fig. 4. Note that of the 500 Monte Carlo cases ran, zero percent skipped out.

Results of the Monte Carlo study for further off-nominal overburns and underburns are shown in Tables 13 - 19. The corresponding Monte Carlo impact points accounting for all three debris fields are coplotted in Figs. 5 - 13.

From the results, it is seen that footprints are definable for burns greater than or equal to 19.5 m/sec, and Figs. 4 - 12 can be thought of as showing an estimated debris footprint.

From Fig. 13, we then see that for a burn of 18.5 m/sec (5 m/sec, or 21%, underburn), debris can fall anywhere along the orbital groundtrack for approximately one orbit. For underburns of 5 m/sec or greater, the intact vehicle is "bouncing" off the upper atmosphere, after entering far enough to shed the solar arrays, with the rest entering at a later, unpredictable time and location. Thus, the true footprint size is indeterminable. Note that for these underburns, there could have been multiple reentries of modules (the initial atmosphere bounce may separate the modules), where each enters in its own underminable location. As such, Fig. 13, which shows impact locations for the 18.5 m/sec burn, should not be thought of as a footprint. In reality, any of the points on this plot could be contained in the actual footprint (or footprints).

Note that of the 500 Monte Carlo cases ran, zero percent skipped out for deorbit burns of 20.5 m/sec and higher. The 19.5 m/sec burn showed small potential for skipout and the 18.5 m/sec and lower burns showed likely skipout.

Table 12. 4 m/sec Overburn MC Results

Statistic	General Debris	All Debris
Length	2640 km	5170 km
Width	440 km	440 km
Center w.r.t. Japan	7820 km	8560 km
Heel w.r.t. Japan	6490 km	5970 km
Toe w.r.t. Chili	8250 km	6250 km
Min Time to 15.24 km	22.9 min	22.1 min
Max Time to 15.24 km	34.5 min	34.5 min

Table 13. 3 m/sec Overburn MC Results

Statistic	General Debris	All Debris
Length	2770 km	5460 km
Width	440 km	440 km
Center w.r.t. Japan	8210 km	8940 km
Heel w.r.t. Japan	6820 km	6200 km
Toe w.r.t. Chili	7800 km	5730 km
Min Time to 15.24 km	23.7 min	22.7 min
Max Time to 15.24 km	35.4 min	35.4 min

Table 14. 2 m/sec Overburn MC Results

Statistic	General Debris	All Debris
Length	2890 km	5800 km
Width	430 km	430 km
Center w.r.t. Japan	8640 km	9350 km
Heel w.r.t. Japan	7190 km	6450 km
Toe w.r.t. Chili	7300 km	5140 km
Min Time to 15.24 km	24.6 min	23.3 min
Max Time to 15.24 km	36.2 min	36.2 min

Table 15. 1 m/sec Overburn MC Results

Statistic	General Debris	All Debris
Length	3030 km	6230 km
Width	420 km	420 km
Center w.r.t. Japan	9140 km	9830 km
Heel w.r.t. Japan	7620 km	6720 km
Toe w.r.t. Chili	6730 km	4450 km
Min Time to 15.24 km	25.6 min	24.0 min
Max Time to 15.24 km	37.3 min	37.3 min

Table 16. 1 m/sec Underburn MC Results

Statistic	General Debris	All Debris
Length	3450 km	7190 km
Width	370 km	370 km
Center w.r.t. Japan	10500 km	10960 km
Heel w.r.t. Japan	8770 km	7360 km
Toe w.r.t. Chili	5170 km	2840 km
Min Time to 15.24 km	28.3 min	25.5 min
Max Time to 15.24 km	40.1 min	40.1 min

Table 17. 2 m/sec Underburn MC Results

Statistic	General Debris	All Debris
Length	3910 km	8030 km
Width	340 km	340 km
Center w.r.t. Japan	11510 km	11770 km
Heel w.r.t. Japan	9560 km	7750 km
Toe w.r.t. Chili	3930 km	1620 km
Min Time to 15.24 km	30.3 min	26.6 min
Max Time to 15.24 km	43.1 min	43.1 min

Table 18. 3 m/sec Underburn MC Results

Statistic	General Debris	All Debris
Length	4780 km	9490 km
Width	300 km	300 km
Center w.r.t. Japan	12950 km	12970 km
Heel w.r.t. Japan	10560 km	8220 km
Toe w.r.t. Chili	2040 km	-360 km
Min Time to 15.24 km	32.8 min	27.8 min
Max Time to 15.24 km	48.9 min	48.9 min

Table 19. 4 m/sec Underburn MC Results

Statistic	General Debris	All Debris
Length	7420 km	13090 km
Width	390 km	390 km
Center w.r.t. Japan	15630 km	15320 km
Heel w.r.t. Japan	11920 km	8770 km
Toe w.r.t. Chili	-1990 km	-4510 km
Min Time to 15.24 km	36.4 min	29.1 min
Max Time to 15.24 km	62.4 min	62.4 min

6. CONCLUSIONS

This paper presented the detailed method and results of Monte Carlo simulations of the Mir Space Station entry, assuming general breakup at 90.0 km, and debris flight to ground impact. Overburn and underburn scenarios were considered in addition to the nominal burn plan. Results showed predictable footprint locations for burns greater than or equal to 19.5 m/sec (or ≤ 4 m/sec underburn). The 4 m/sec underburn case showed small potential for skipout. A 5 m/sec underburn was found to be borderline skipout, with debris impact potential for approximately one orbit. Larger underburns were not studied, as it skipout was assumed with potential for multiple reentries of modules in unpredictable locations. All primary results are summarized in Tables 11 – 19 and Figs. 1 - 13.

7. FUTURE MODELING CHANGES

Future model updates will include added capabilities to model breakup over an altitude range, and explosive breakups. The crossrange calculation will be modified to be relative to the entry groundtrack, not the orbital groundtrack frozen at the initial state vector time.

Fig. 1. Nominal Final Burn MC Impact Points - All Three Debris Fields

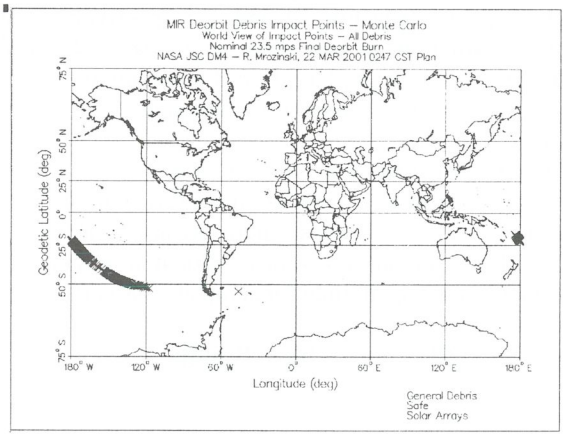

Fig. 2. Eastern Hemisphere Break-off and Breakup Location Estimates

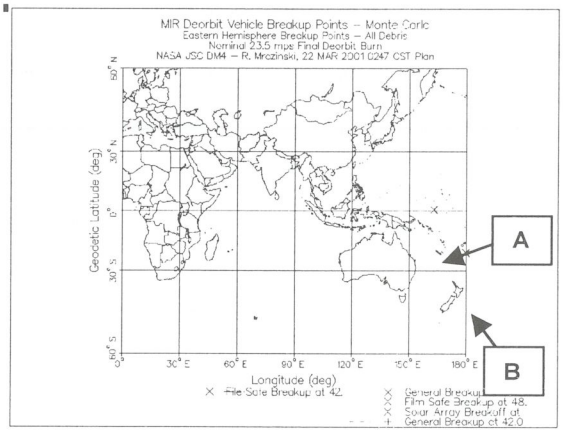

Fig. 3. Western Hemisphere Break-off and Breakup Location Estimates

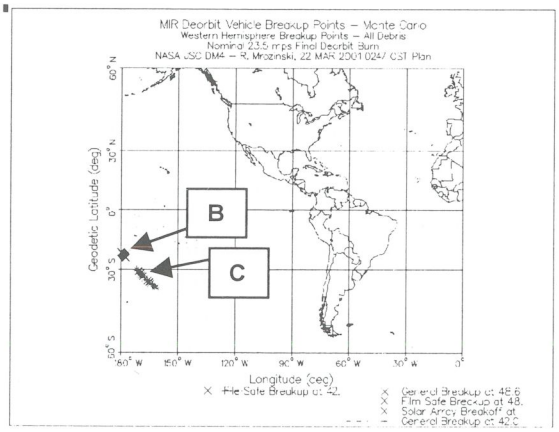

Fig. 4. Off-Nominal 4 m/sec Overburn MC Impact Points - All Three Debris Fields

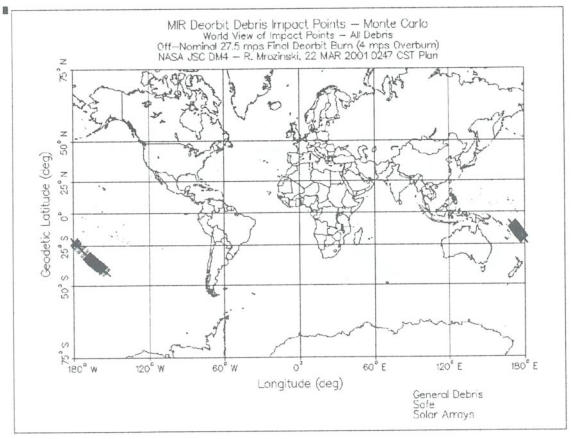

Fig. 5. Off-Nominal 3 m/sec Overburn MC Impact Points - All Three Debris Fields

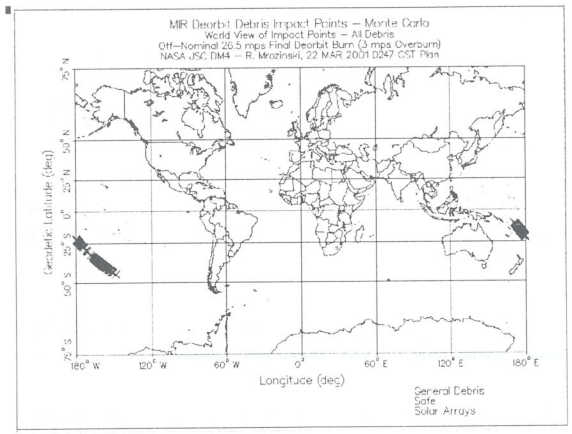

Fig. 6. Off-Nominal 2 m/sec Overburn MC Impact Points - All Three Debris Fields

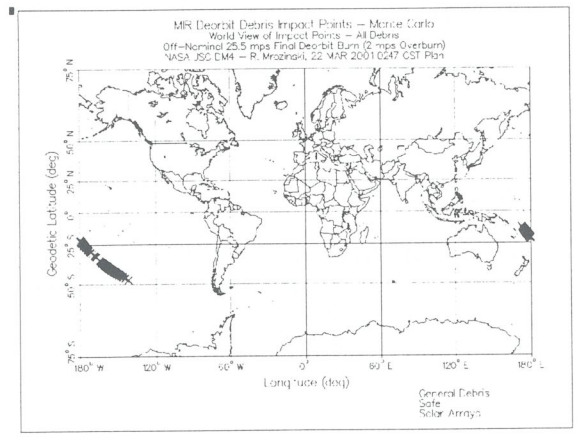

Fig. 7. Off-Nominal 1 m/sec Overburn MC Impact Points - All Three Debris Fields

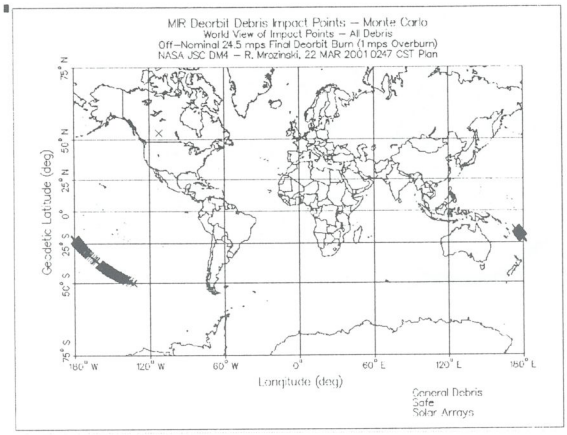

Fig. 8. Nominal Final Burn MC Impact Points - All Three Debris Fields (Repeated Here for Completeness)

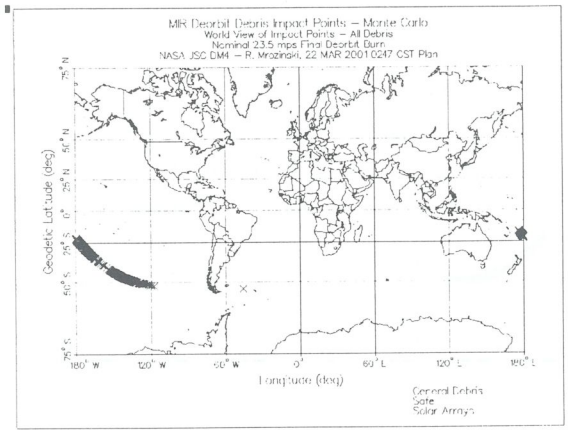

Fig. 9. Off-Nominal 1 m/sec Underburn MC Impact Points - All Three Debris Fields

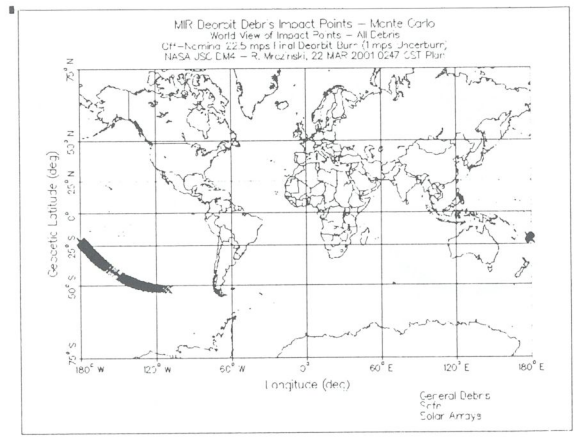

Fig. 10. Off-Nominal 2 m/sec Underburn MC Impact Points - All Three Debris Fields

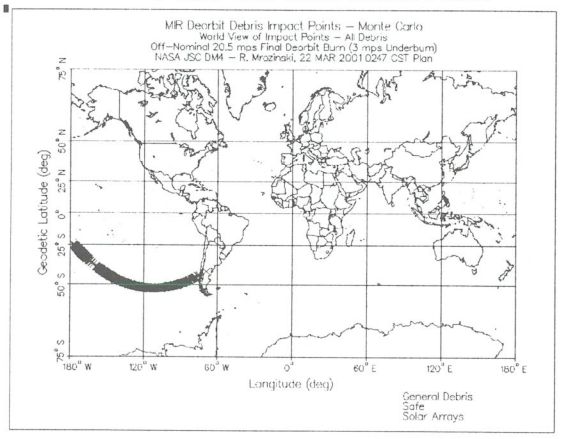

Fig. 11. Off-Nominal 3 m/sec Underburn MC Impact Points - All Three Debris Fields

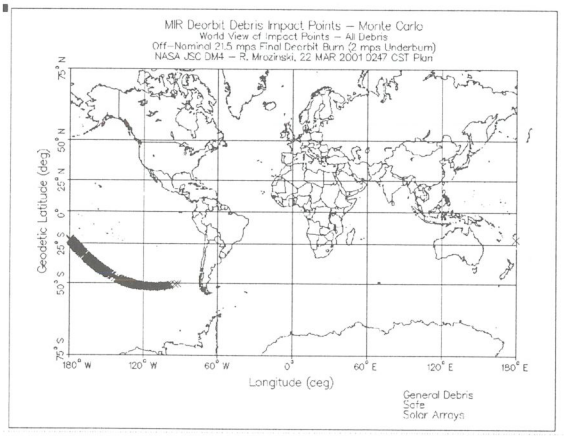

Fig. 12. Off-Nominal 4 m/sec Underburn MC Impact Points - All Three Debris Fields

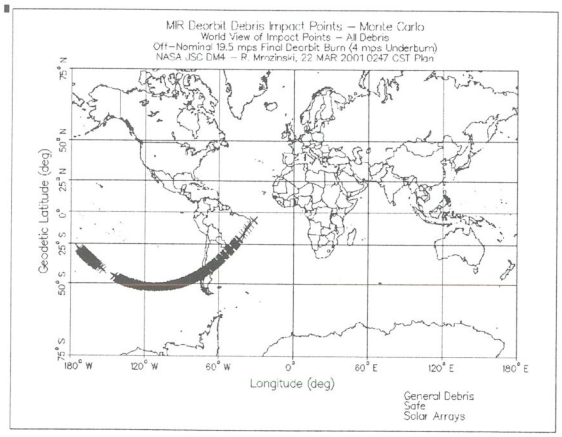

Fig. 13. Off-Nominal 5 m/sec Underburn MC Impact Points - All Three Debris Fields

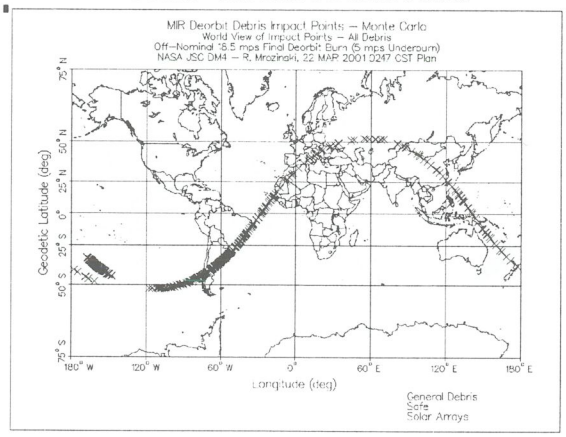

8. REFERENCES

1. Berning, M. J., Sagis, K. D., "User's Guide for the Simulation and Optimization of Rocket Trajectories (SORT) Program, Version 7," NAS9-17900, Lockheed Engineering & Sciences Company, Houston, Texas, October, 1992.

2. Rao, P. P., Woeste, M. A., "Monte Carlo Analysis of Satellite Debris Footprint Dispersion," AIAA 79-1628, 1979.

3. Cerimele, C. J., conversation, NASA Johnson Space Center, Houston, Texas, May 03, 2000.

4. Mrozinski, R. B., "CRV Deorbit Opportunities, v1.0h," unpublished, NASA Johnson Space Center, Houston, Texas, January 24, 2000.

5. Paul, S. D., "Mir: Final Plan of Action," e-mail communication, NASA Johnson Space Center, Houston, Texas, March 21, 2001.

6. Paul, S. D., "Final Plan," e-mail communication, NASA Johnson Space Center, 0247 CST, Houston, Texas, March 22, 2001.

7. Ivanov, N. M., Kudriavtsev, S. I., Udaloy, V. A., Blagov, V. D., "Flight Dynamics and Navigation Support Features of Last Stage of MIR Flight," Russian Mission Control Centre, Korolev, Russia, undated.

8. "Reply to Questions Posed by the U. S. Government in a Letter of January 26, 2001, Regarding the De-Orbit of Mir," translated facsimile transmission, February 06, 2001.

9. Martirosov, M., conversation, Mir Deorbit Technical Interchange Meeting, NASA Johnson Space Center, Houston, Texas, February 08, 2001.

10. McCormick, P. O., e-mail communications, Lockheed Martin, January 2000.

11. Herdrich, R. J., Nguyen, P. D., "Super Lightweight Tank (SLWT) Footprint Analysis: Technical Report," JSC-27712, NASA Johnson Space Center, Houston, Texas, March 01, 1997.

12. Loftus Jr., J. P., conversation, NASA Johnson Space Center, Houston, Texas, January 31, 2000.

13. Cole, C. E., "Gamma Ray Observatory Mission Contract, Observatory Reentry Plan (Final)," DRL 023, 40420-85-023-001, TRW Space & Technology Group, Federal Systems Division, July 31, 1985.

14. Refling, O., Stern, R., Potz, C., "Review of Orbital Reentry Risk Predictions," Aerospace Report No. ATR-92(2835)-1, Programs Group, The Aerospace Corporation, El Segundo, California, July 15, 1992.

15. Brown-Conwell, E. R., "GRO Mission Flight Dynamics Analysis Report: Controlled Reentry of the Gamma Ray Observatory," CSC/TM-90/6001, Mission Report 90001, Flight Dynamics Division, NASA Goddard Space Flight Center, Greenbelt, Maryland, November 1989.

16. Loftus Jr., J. P., "Reentry of the Compton Gamma Ray Observatory," presentation, NASA Johnson Space Center, Houston, Texas, October 12, 2000.

17. Kennedy, "COPUOS: Russian Paper On Mir Space Station Deorbit," Telegram Ref: A. UNVIE VIENNA 273 B. SECSTATE 25241, USMISSION UNVIE VIENNA (UNVIE VIEN 281 – ROUTINE), February, 14, 2001.

18. Scheffe, H., Tukey, J. W., "A Formula for Sample Sizes for Population Tolerance Limits," *Annals of Mathematical Statistics*, Vol. 15, p. 217, 1944.